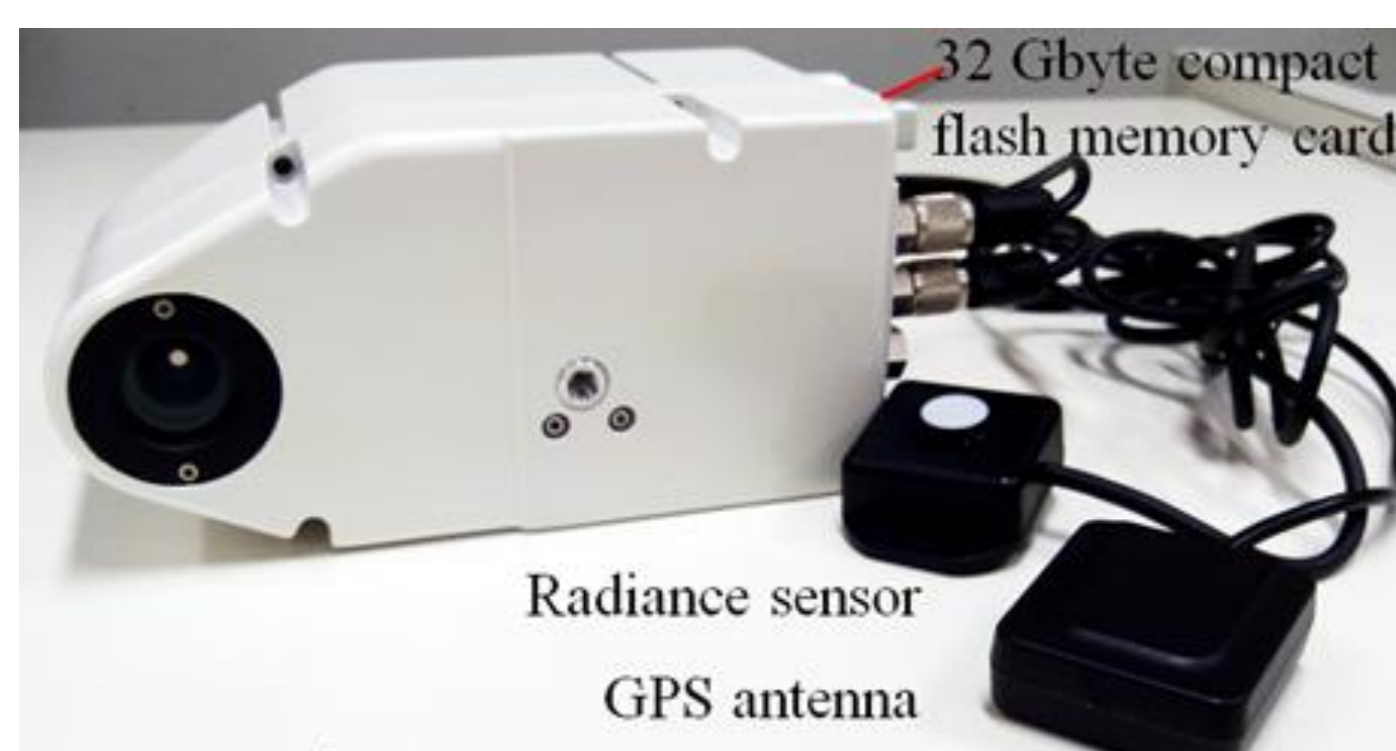


INTRODUCTION

The lightweight hyperspectral camera based on a Fabry-Pérot interferometer (FPI) is one of the highly interesting tools for UAV based remote sensing for environmental and agricultural applications. The camera used in this study acquires images from different wavelengths by changing the FPI gap and using two CMOS sensors. Due to the acquisition principle of this camera, the interior orientation parameters (IOP) of the spectral bands can vary for each band and sensor and changing the configuration also would change these sets of parameters posing an operational problem when several bands configurations are being used. The objective of this study is to assess the impact of use IOPs estimated for some bands in one configuration for other bands of different configuration the FPI camera, considering different IOP and EOP constraints. The experiments were performed with two FPI-hyperspectral camera data sets: the first were collected 3D terrestrial close-range calibration field and the second onboard of an UAV.

HYPERSPECTRAL IMAGING WITH UAV

- Advantages: flexibility; favourable cost-benefit ratio and high-temporal resolution;
- Several problems require multi/hyperspectral images;
- Orientation data have to be acquired during the flight using GNSS and IMU;
- Hyperspectral sensors usually have pushbroom geometry;
 - Alternative – hyperspectral frame cameras.



Horizontal FOV	37°
Vertical FOV	37°
Spectral range	500 nm - 900 nm
Spectral Resolution	10 nm (FWHM)*
F-number	~2,8
Sensors	CMOS - CMV400
Images dimensions	1023 x 648 pixels
Pixel size	5.5 µm x 5.5 µm
Principal distance	8.7 mm
Weight	~ 700 g

- Light-weight hyperspectral frame camera developed by VTT using a Fabry-Perot interferometer (FPI);
- The sensor spectral sensitivity is a function of the interferometer air gap;
- The same principle is being used by Rikola;
- Some camera models have two sensors.

Hyperspectral camera – key problems

- Determination and stability of IOPs;
- Determination of EOPs;
- Bands registration;
- Unfeasible to define a single set of IOPs for this camera;
- Some reference bands can be chosen and their IOPs, estimated by calibration, could be used for the remaining bands;

- Use On-the-Job calibration to cope with instability.

Hyperspectral camera – Determination of EOPs

- Directly, by using GNSS and INS;
- Indirectly, by Bundle Adjustment;
- Integrated Sensor Orientation (ISO);
- In any case, rigorous sensor modeling is required;
- It cannot be ensured that the IOPs determined by laboratory or terrestrial techniques are stable;
- It is unfeasible to generate IOPs for all possible sets of configurations that can be tested and used in a surveying;
- With IOPs variations, the results of BBA or ISO are likely to be affected.

Band	λ (nm)	Band	λ (nm)	Band	λ (nm)	Band	λ (nm)
1	506.07	14	680.06	1	506.07	14	680.06
2	520.00	15	689.56	2	520.00	15	689.56
3	535.45	16	699.62	3	535.45	16	699.62
4	550.76	17	709.71	4	550.76	17	709.71
5	564.71	18	719.99	5	564.71	18	719.99
6	580.08	19	729.56	6	580.08	19	729.56
7	591.49	20	740.45	7	591.49	20	740.45
8	605.64	21	749.65	8	605.64	21	749.65
9	619.55	22	770.46	9	619.55	22	770.46
10	629.93	23	790.21	10	629.93	23	790.21
11	650.28	24	810.15	11	650.28	24	810.15
12	660.27	25	829.93	12	660.27	25	819.70
13	669.96			13	669.96		

(cfg. 2) used in the terrestrial calibration (cfg. 1) used in flight

Terrestrial camera calibration

- Calibration was performed for both sensors using a reference spectral band for each sensor;
- Camera was configured with the cfg. 2 and calibrated considering two reference bands for each sensor (band 8 for sensor 2 and band 23 for sensor 1);
- Additional calibrations trials were performed for more two bands of the sensor 1 (bands 15 and 22);
- 12 cubes were acquired with different positions and rotations;
- The reference frame for the self-calibration with bundle adjustment was defined by the 3D coordinates of two points and the Z coordinate (depth) of a third point.

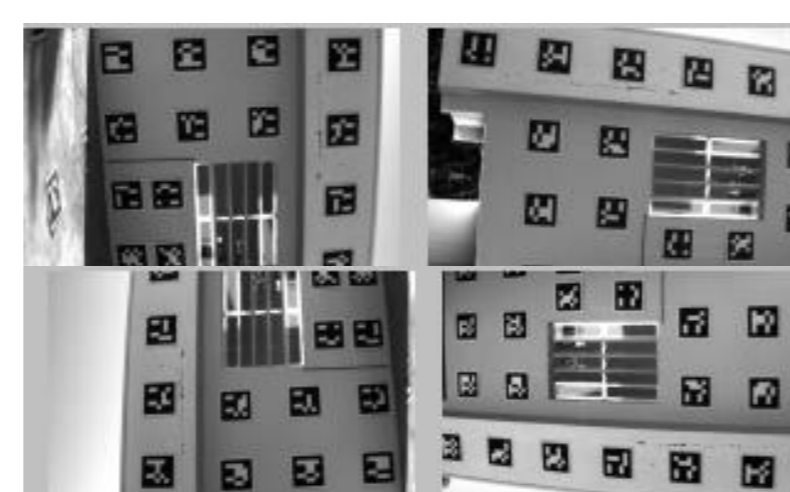


Image bands used for terrestrial calibration

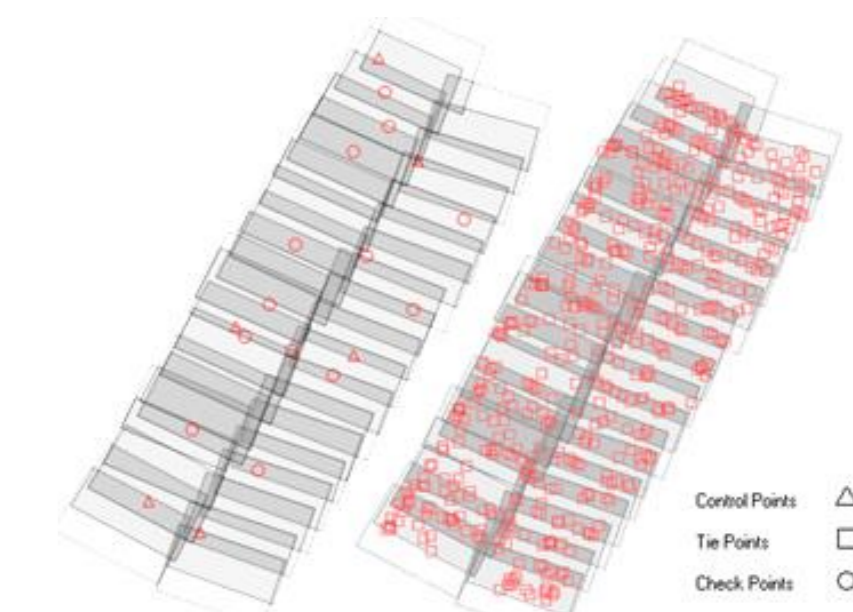
- Standard deviations (images) = 0.5 pixel;
- Experiments with 8 parameters:
 - (c, x0, y0, k1, k2, k3, P1, P2);
- Results achieved for sensor 1 > sensor 2
 - Explained by the image quality: images from sensor 2 are more blurred probably due to the beam splitting optics.

Check distances for each set of bands IOPs

Band id	8	15	22	23
Number of distances	15	16	16	16
Mean error (mm)	-0.705	-0.027	-1.104	-0.822
	± 4.521	± 4.421	± 4.043	± 4.182
RMSE (mm)	4.424	4.280	4.067	4.131
Minimum error (mm)	1.692	1.739	0.313	0.077
Maximum error (mm)	8.184	7.87	7.318	7.21

EXPERIMENTS WITH UAV IMAGES

- 2 flight strips - 360 m;
- Flight height of 90 m;
- GSD of 6 cm;
- Forward overlap was 60%;
- Side overlap of 10-20 %;
- 6 GCP and 13 check points;
- 2 bands of cfg. 1 were used;
- GPS time for each event of cube acquisition (first band);
- Acquisition time of the remaining bands were estimated by the nominal time differences (22 ms);
- Double frequency GNSS receiver grabbed raw data - 1 Hz;
- The position of each image band was interpolated from these data and used as observations in the bundle adjustment.



Results for aerial images of band 8 with IOPs of band 8 from terrestrial calibration

	BBA 1	BBA 2	OJC
$\sigma_{IOP}(C, X_0, Y_0)$	fixed	fixed	15 µm
$\sigma_{PC}(m)$	unknown-	0.2	0.2
A posteriori σ	0.386	0.638	0.441
RMSE X (m)	0.246	0.281	0.217
RMSE Y (m)	0.259	0.423	0.266
RMSE Z (m)	0.469	1.232	0.562

Results for aerial images of band 23 with IOPs of band 22 from terrestrial calibration

	BBA 1	BBA 2	OJC
$\sigma_{IOP}(C, X_0, Y_0)$	fixed	fixed	15 µm
$\sigma_{PC}(m)$	unknown-	0.2	0.2
A posteriori σ	0.449	0.734	0.509
RMSE X (m)	0.261	0.293	0.238
RMSE Y (m)	0.194	0.154	0.129
RMSE Z (m)	0.639	0.967	0.527

Results for aerial images of band 23 with IOPs of band 23 from terrestrial calibration

	BBA 1	BBA 2	OJC
$\sigma_{IOP}(C, X_0, Y_0)$	fixed	fixed	15 µm
$\sigma_{PC}(m)$	unknown-	0.2	0.2
A posteriori σ	0.446	0.721	0.505
RMSE X (m)	0.259	0.290	0.236
RMSE Y (m)	0.191	0.150	0.129
RMSE Z (m)	0.650	0.930	0.524

Results for aerial images of band 23 with IOPs of band 15 from terrestrial calibration

	BBA 1	BBA 2	OJC
$\sigma_{IOP}(C, X_0, Y_0)$	fixed	fixed	15 µm
$\sigma_{PC}(m)$	unknown-	0.2	0.2
A posteriori σ	0.445	0.727	0.506
RMSE X (m)	0.260	0.290	0.235
RMSE Y (m)	0.191	0.154	0.129
RMSE Z (m)	0.674	0.994	0.530

CONCLUSIONS

- To assess the use of a lightweight FPI hyperspectral camera with photogrammetric techniques;
- Determination of the IOPs and its change with different bands configurations;
- Experiments with some reference bands of two sensors were performed both with terrestrial and aerial data;
- Flight configurations were not optimal:
 - side overlap;
 - one flight height.
- The results have shown that some IOPs have to be estimated on-the-job with bundle adjustment to provide suitable results;
- Further research is needed to assess the stability of the camera inner orientation and the use of IOP values of some reference bands.

IOPs estimated in terrestrial and on-the-job calibration (OJC) band 23

Location	Terrestrial	OJC	OJC	OJC
Band id	23	23	22	15
c(mm)	8.7000	8.7491	8.7499	8.7500
x ₀ (mm)	0.4084	0.2787	0.2747	0.2850
y ₀ (mm)	0.4006	0.2215	0.2186	0.2189

REFERENCE

Tommaselli, A. M. G., Berveglieri, A., Oliveira, R. A., Nagai, L. Y. and Honkavaara, E. Orientation and calibration requirements for hyperspectral imaging using UAVs: a case study. *ISPRS - Int. Arch. Photogramm. Remote Sens. Spat. Inf. Sci.*, vol. XL-3/W4, pp. 109–115, 2016.